

Observation of nuclear dechanneling length reduction for high energy protons in a short bent crystal



W. Scandale^{a,b,e}, G. Arduini^a, M. Butcher^a, F. Cerutti^a, M. Garattini^a, S. Gilardoni^a, L. Lari^{a,k}, A. Lechner^a, R. Losito^a, A. Masi^a, A. Mereghetti^a, E. Metral^a, D. Mirarchi^{a,j}, S. Montesano^a, S. Redaelli^a, R. Rossi^{a,e}, P. Schoofs^a, G. Smirnov^a, E. Bagli^c, L. Bandiera^c, S. Baricordi^c, P. Dalpiaz^c, G. Germogli^c, V. Guidi^c, A. Mazzolari^c, D. Vincenzi^c, G. Claps^d, S. Dabagov^{d,l}, D. Hampai^d, F. Murtas^d, G. Cavoto^e, F. Iacoangeli^e, L. Ludovici^e, R. Santacesaria^e, P. Valente^e, F. Galluccio^f, A.G. Afonin^g, Yu.A. Chesnokov^g, V.A. Maishev^g, Yu.E. Sandomirskiy^g, A.A. Yanovich^g, I.A. Yazynin^g, A.D. Kovalenko^h, A.M. Taratin^h, Yu.A. Gavrikovⁱ, Yu.M. Ivanovⁱ, L.P. Lapinaⁱ, W. Ferguson^j, J. Fulcher^j, G. Hall^j, M. Pesaresi^j, M. Raymond^j, D. Bolognini^{m,n}, S. Hasan^{m,n}, M. Prest^{m,n}, E. Vallazza^o

^a CERN, European Organization for Nuclear Research, CH-1211 Geneva 23, Switzerland

^b Laboratoire de l'Accélérateur Lineaire (LAL), Université Paris Sud Orsay, Orsay, France

^c INFN Sezione di Ferrara, Dipartimento di Fisica, Università di Ferrara, Ferrara, Italy

^d INFN LNF, via E. Fermi 40, 00044 Frascati (Roma), Italy

^e INFN Sezione di Roma, Piazzale Aldo Moro 2, 00185 Rome, Italy

^f INFN Sezione di Napoli, Italy

^g Institute of High Energy Physics, Moscow Region, RU-142284 Protvino, Russia

^h Joint Institute for Nuclear Research, Joliot-Curie 6, 141980 Dubna, Moscow Region, Russia

ⁱ Petersburg Nuclear Physics Institute, 188300 Gatchina, Leningrad Region, Russia

^j Imperial College, London, United Kingdom

^k Instituto de Física Corpuscular (CSIC-IFIC), Valencia, Spain

^l P.N. Lebedev Physical Institute & NRNU MEPhI, Moscow, Russia

^m Università dell'Insubria, via Valleggio 11, 22100 Como, Italy

ⁿ INFN Sezione di Milano Bicocca, Piazza della Scienza 3, 20126 Milano, Italy

^o INFN Sezione di Trieste, Via Valerio 2, 34127 Trieste, Italy

ARTICLE INFO

Article history:

Received 8 December 2014

Received in revised form 16 February 2015

Accepted 28 February 2015

Available online 5 March 2015

Editor: L. Rolandi

Keywords:

Crystal
Channeling
Beam
Deflection

ABSTRACT

Deflection of 400 GeV/c protons by a short bent silicon crystal was studied at the CERN SPS. It was shown that the dechanneling probability increases while the dechanneling length decreases with an increase of incident angles of particles relative to the crystal planes. The observation of the dechanneling length reduction provides evidence of the particle population increase at the top levels of transverse energies in the potential well of the planar channels.

© 2015 The Authors. Published by Elsevier B.V. This is an open access article under the CC BY license (<http://creativecommons.org/licenses/by/4.0/>). Funded by SCOAP³.

When high energy charged particles enter a crystal with small angles relative to the crystal planes, $\theta_0 \ll 1$, their motion is governed by a crystal potential, $U(x)$, averaged along the planes [1]. If the angles are smaller than the critical angle $\theta_0 < \theta_c =$

$(2U_0/pv)^{1/2}$, where p , v are the particle momentum and velocity, respectively, and U_0 is the well depth of the averaged planar potential, the particles can be captured into the channeling regime. Channeled particles move in a crystal oscillating between two neighboring planes. Channeling is also possible in a bent crystal if

E-mail address: alexander.taratin@cern.ch (A.M. Taratin).

its bend radius is larger than the critical value, $R > R_c = pv/eE_m$ [2], where E_m is the maximum strength of the electric field in the planar channel. In a bent crystal, the particle motion is governed by the effective potential $U_{eff}(x, R) = U(x) + x \cdot pv/R$.

The averaged planar potential provides an approximate description of channeling, in which the transverse energy of particles is the integral of motion. Incoherent (multiple and single) scattering by the crystal electrons and nuclei changes the transverse energy of channeled particles and they leave the channels, that is dechanneling occurs. The density of atomic nuclei reduces quickly with the distance x from the planes according to a Gaussian distribution $P_n(x) \sim \exp(-x^2/u_\perp^2)$, where $u_\perp = \sqrt{2}u_1$ and u_1 is the amplitude of thermal vibrations of the crystal atoms. Therefore, the dechanneling process has two stages for most of channeled particles entering the crystal sufficiently far from the channel walls. In the first slow stage particles increase their transverse energy due to multiple scattering on the crystal electrons. The experimental data [3] have shown that a good approximation for the critical approach distance to the channel walls is $r_c = 2.5u_1$ where the fast dechanneling stage due to multiple scattering by atomic nuclei begins (“nuclear corridor”). The value of the planar potential at the distance r_c determines the critical transverse energy for the stable channeling states $E_{xc} = U_{eff}(x = r_c)$. The dechanneling process has an exponential character in the first approximation, $N_{ch}(z) \sim \exp(-z/S_d)$, where S_d is the dechanneling length. The dechanneling length measured in the experiment [4] is about 10 cm for 200 GeV/c protons in the (110) channels of a 44 mm long straight silicon crystal. It determines the reduction of particles in the stable channeling states due to multiple scattering on the crystal electrons, the electron dechanneling length S_e . The dechanneling length is approximately proportional to the particle energy.

Short crystals with length $L \ll S_e$ are required to study the fast mechanism of nuclear dechanneling. The crystal bend provides the angular unfolding of the dechanneling process. The first measurement of the nuclear dechanneling length was realized in the experiment [5] using a 2 mm long silicon crystal bent along the (110) planes with a bend radius $R = 40$ m for 400 GeV/c protons. The measured nuclear dechanneling length was about 1.5 mm which is more than 100 times smaller than the electron dechanneling length for this energy of protons.

It should be noted that for the planar channeling of negative particles nuclear multiple scattering is the main mechanism of dechanneling because all the particles oscillate around the crystal planes. The dechanneling length for 150 GeV/c π^- mesons was measured in the experiment [6]. Its value, $S_n \approx 1$ mm, is the same order of magnitude as the nuclear dechanneling length for positive particles with the same energy.

Fig. 1 shows the effective potential $U_{eff}(x, R)$ in the silicon crystal bent along the (110) planes with the radius $R = 10.26$ m for 400 GeV/c protons. The interval of transverse energies (E_{xc}, E_{xm}), where $E_{xm} = U_{eff}(0, R)$ is the potential well depth, determines the particle fraction undergoing dechanneling due to strong multiple scattering by the crystal nuclei. One would expect that dechanneling should be faster for particles when their transverse energy is closer to the well depth E_{xm} . The number of such near-barrier particles should increase with an increase of the beam orientation angle relative to the planes at the crystal entrance.

In this paper, the results of the experiment at the CERN SPS on the deflection of 400 GeV/c protons by a short bent silicon crystal are considered. The analysis of different beam fractions for the crystal orientation optimal for channeling allows to observe the reduction of the nuclear dechanneling length with an increase of the orientation angle of the considered beam fraction relative to the planes at the crystal entrance.

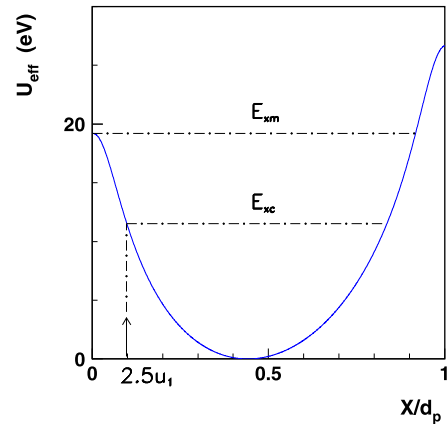


Fig. 1. (Color online.) The effective potential $U_{eff}(x, R)$ in the bent silicon crystal for 400 GeV/c protons as a function of a relative coordinate x/d_p , where $d_p = 1.92$ Å is the distance between two planes. The crystal is bent along the (110) planes with the radius $R = 10.26$ m. Here E_{xm} is the maximal transverse energy for channeled particles, $E_{xm} = U_{eff}(0, R)$ is the potential well depth, E_{xc} is the critical transverse energy for stable channeling, $E_{xc} = U_{eff}(x = 2.5u_1)$. The interval (E_{xc}, E_{xm}) determines the range where dechanneling of particles occurs due to multiple scattering by the atomic nuclei of the crystal.

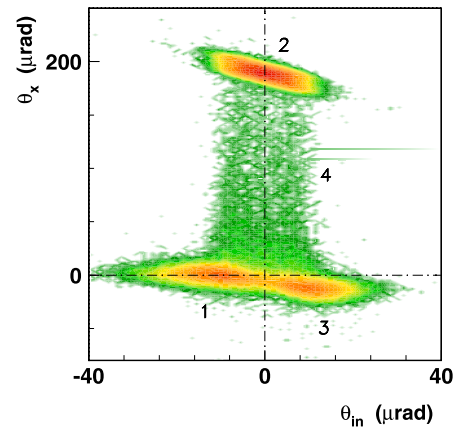


Fig. 2. (Color online.) The intensity distribution of 400 GeV/c protons passed through the bent silicon crystal when its orientation is optimal for channeling in the deflection angles θ_x as a function of incidence angle θ_{in} of particles relative to the (110) planes at the crystal entrance.

The experimental setup was the same described in [7]. Four microstrip silicon detectors, two upstream and two downstream of the crystal, were used to detect the particle trajectories with an angular resolution of $3 \mu\text{rad}$, which is limited by the multiple scattering of particles in the detectors and air. A $70 \times 1.94 \times 0.5 \text{ mm}^3$ silicon strip crystal with the largest faces parallel to the (110) crystallographic planes was fabricated according to the methodology described in [8,9]. The strip-crystal was bent along its length and placed vertically, so that the induced anticlastic bending along the crystal width was used to deflect particles in the horizontal plane (see Fig. 2b in [7]). The beam of 400 GeV/c protons had the RMS value of the horizontal angular divergence of $\sigma_x = (9.34 \pm 0.06) \mu\text{rad}$. A high precision goniometer, with an accuracy of $2 \mu\text{rad}$, was used to orient the (110) crystal planes parallel to the beam direction. An angular scan was performed and the optimal orientation was found, which gives the maximum of the deflected beam fraction.

Fig. 2 shows the intensity distribution of 400 GeV/c protons passed through the bent silicon crystal when its orientation is optimal for channeling in the deflection angles θ_x as a function of incidence angle θ_{in} of particles relative to the (110) plane at

the crystal entrance. The beam divergence value allows to observe the different interaction mechanisms with the crystal for the different beam fractions. The fraction 1 consists of the particles passed through the crystal which experienced the same multiple scattering as in the amorphous substance. The particles which passed the full length of the crystal in the channeling regime and deflected by the bend angle represent the fraction 2. The fraction 3 consists of the particles deflected to the side opposite to the crystal bend due to volume reflection. The dechanneled particles, which are found in the angular interval between the initial direction and that of the channeled fraction, represent the fraction 4.

Let us consider the different beam fractions with the incident angles $\theta_{in} \pm \Delta\theta_{in}$, where $\Delta\theta_{in} = 1.75 \mu\text{rad}$. Fig. 3a shows the deflection angle distribution of protons for the optimal case when $\theta_{in} = 0$. The peak on the right consists of the particles passed through the whole crystal in the channeling regime. The peak has a well visible central part because the considered fraction of the incident beam consists of particles with all transverse energies satisfying the channeling conditions including the smallest ones. The maximum of the peak is at an angle $\theta_{ch} = 189 \mu\text{rad}$ and its position corresponds to the crystal bend angle $\theta_{ch} = \alpha$. The part of particles deflected by the angles larger than $\theta_{ch} - 3\sigma_{ch}$ (the boundary is shown by the dot-dashed line), where σ_{ch} is the RMS deviation of a Gaussian fit of the peak, determines the deflection (channeling) efficiency, it is $P_{ch} = 77\%$. The peak on the left is formed by the particles, which were not captured into the channeling regime. The peak is shifted to the side opposite to the crystal bend by the angle of θ_{VR} due to volume reflection. The peak boundary at $\theta_{VR} + 3\sigma_{VR}$, where σ_{VR} is the RMS deviation of a Gaussian fit of this peak, is shown by the dot-dashed line.

The particles with deflection angles within the angular interval indicated in Fig. 3 by two dot-dashed lines are the dechanneled ones N_{dc} . The particle deflection angle is determined by the distance S passed in the channeling regime, $\theta_{xs} = S/R$. The total number of particles in the channeling peak and the dechanneling region represents those particles captured into the channeling regime at the crystal entrance $N_{ch}(0)$. The dechanneling probability is defined as the ratio $P_{dc} = N_{dc}/N_{ch}(0)$. For the case under consideration, $P_{dc} = 7.2\%$. The solid line shows an exponential fit of the central dechanneling region, which gives the dechanneling length value, $S_n = 1.38 \pm 0.24 \text{ mm}$.

Fig. 3b shows the distribution of deflection angles for the beam fraction with an incident angle $\theta_{in} = 8.75 \mu\text{rad}$, which is close to the critical channeling angle, $\theta_{cb}(R) = 9.8 \mu\text{rad}$, for the considered bend radius R . In this case, the channeling peak is additionally shifted because of the angle θ_{in} relative to the planes at the crystal entrance. The upper part of the peak becomes more flat because the number of particles with small oscillation amplitudes decreases (the simulations actually show the two-headed peak, which is also just visible here). The dechanneling probability becomes significantly higher, $P_{dc} = 23.5\%$ and the dechanneling length becomes smaller, $S_n = 0.81 \pm 0.09 \text{ mm}$.

Fig. 4 shows the experimental dependence of the dechanneling probability of 400 GeV/c protons on the incident angle of the beam fraction θ_{in} . The dechanneling probability increases monotonously with increasing θ_{in} . The dependence becomes close to linear for large orientation angles. Fig. 5 shows the dependence of the dechanneling length of protons on the incident angle θ_{in} . The dechanneling length decreases approximately by a factor of two in the angular range considered.

Simulation of the proton beam passage through the bent silicon crystal for the conditions of the considered experiment has been carried out using the CRYD model suggested in [10]. The proton trajectories were found by numerical solution of the equations of

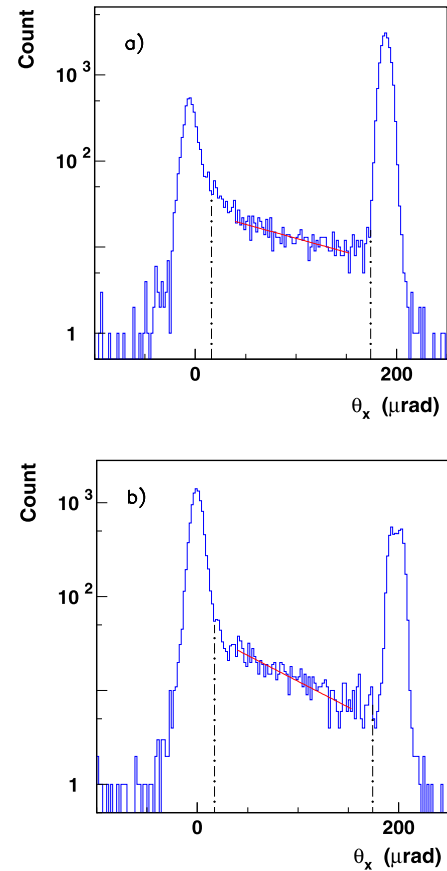


Fig. 3. (Color online.) The distributions of deflection angles for 400 GeV/c protons in the silicon crystal bent along (110) planes for the beam fractions with the incident angles $\theta_{in} \pm \Delta\theta_{in}$, where $\Delta\theta_{in} = 1.75 \mu\text{rad}$. (a) for $\theta_{in} = 0$, (b) for $\theta_{in} = 8.75 \mu\text{rad}$. The channeling peak is on the right. The distribution of dechanneled particles is located between two dot-dashed lines. The solid line shows the exponential fit, which determines the dechanneling length.

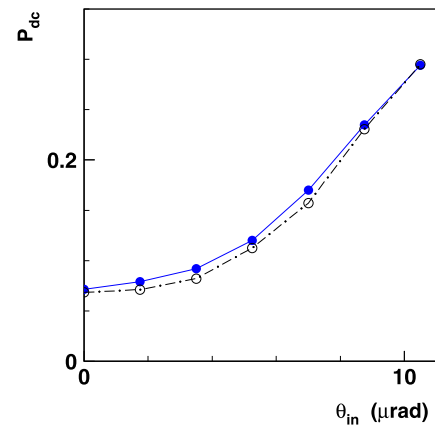


Fig. 4. (Color online.) The experimental dependence of the dechanneling probability of 400 GeV/c protons in the bent silicon crystal on the incident angle of the beam fraction θ_{in} (filled circles). The simulation results are shown by the empty circles and dot-dashed line.

motion in the effective bent planar potential. The change of the transverse velocity of a particle due to multiple scattering on the crystal electrons and nuclei was calculated using the realistic distributions of electrons and nuclei in each step along the trajectory, which was much smaller than the spatial period of the particle oscillations in the planar channels. The calculated dependence of the dechanneling probability is shown by the dot-dashed line in Fig. 4.

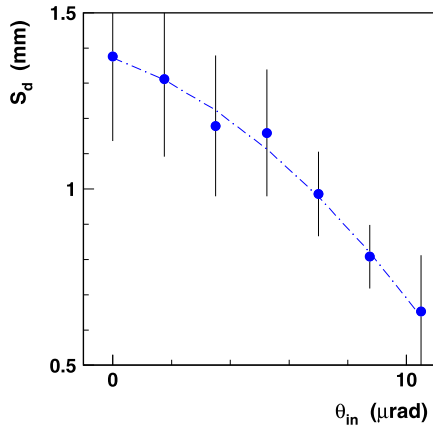


Fig. 5. (Color online.) The dependence of the dechanneling length of 400 GeV/c protons in the bent silicon crystal on the incident angle of the beam fraction θ_{in} .

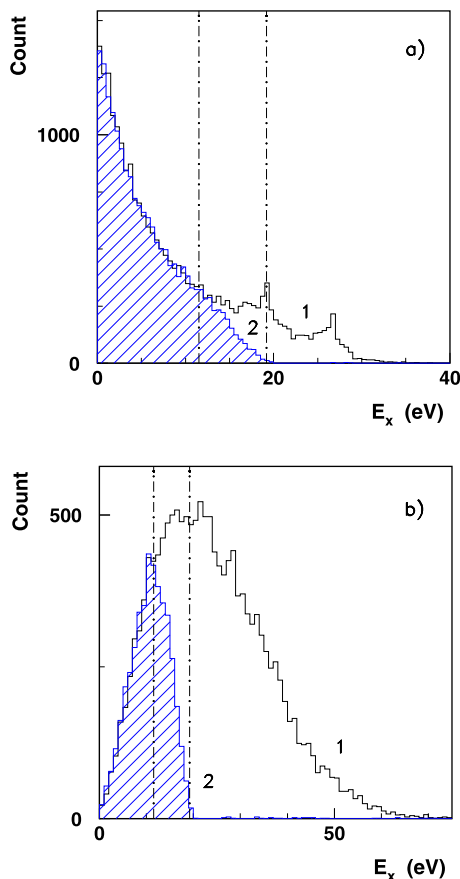


Fig. 6. (Color online.) The calculated particle distributions in the transverse energy E_x at the crystal entrance (1) and exit (2) for the different beam fractions with the incident angles $\theta_{in} \pm \Delta\theta_{in}$, where $\Delta\theta_{in} = 1.75 \mu\text{rad}$. (a) for $\theta_{in} = 0$, (b) for $\theta_{in} = 8.75 \mu\text{rad}$.

The dependence is in good agreement with the experiment, the discrepancy is not larger than 10%.

Fig. 6 shows the calculated particle distributions in the transverse energy E_x at the crystal entrance (1) and exit (2) for the same angles of the beam fraction orientation as in Fig. 3. In the case of $\theta_{in} = 0$ (Fig. 6a) the distribution has a large peak near $E_x = 0$ and two small peaks for the transverse energies corresponding to the effective potential values at the channel walls where its changes are minimal. Two dot-dashed lines show the range of transverse energies at which particles can enter the nu-

clear corridor of the channels. The initial distribution of particles in this range of nuclear dechanneling is approximately uniform. In the case of $\theta_{in} = 8.75 \mu\text{rad}$ the initial distribution in E_x is significantly wider. The distribution maximum is near E_x , which is close to the potential well depth of the planar channel. The distribution of particles in the nuclear dechanneling range of E_x is strongly non-uniform. The particle density with the transverse energies close to the potential well depth value is maximal.

Simulation for protons with transverse energies from narrow layers with the width of 1 eV was made to estimate the dechanneling rate of particles with different E_x from the nuclear dechanneling range (E_{xc}, E_{xm}). The dechanneling lengths for $E_x = 15$ eV and 18 eV, which correspond to the middle and the upper part of the nuclear dechanneling range, were found to be $S_n = 1.49$ mm and 0.61 mm, respectively. The last value is close to the dechanneling length observed in the experiment for the beam fraction with the large incident angle, $\theta_{in} = 10.5 \mu\text{rad}$.

Thus, when the beam fraction enters the crystal at an angle relative to the planes close to the critical one, the population of the upper part of the nuclear dechanneling range is maximal and only those particles determine the dechanneling length value observed in the experiment. The distributions of particle transverse energies at the crystal exit clearly show that dechanneling occurs only from the nuclear corridor range.

The experiment showed that the dechanneling probability increases with an increase of the incident angle of particles relative to the planes which can be explained by the increase of the particle population in the whole range of nuclear dechanneling. Moreover, the observation of the dechanneling length reduction provides evidence of an increase of the particle population at the top part of this nuclear dechanneling range. It is important to take these changes of dechanneling length for protons into account for experiments on the collider beam halo collimation with using bent crystals.

Acknowledgements

We wish to acknowledge the strong support of the CERN EN-STI and BE-AOP groups. We also acknowledge the partial support by the Russian Foundation for Basic Research Grants 05-02-17622 and 06-02-16912, the RF President Foundation Grant SS-3383.2010.2, the LHC Program of Presidium of Russian Academy of Sciences and the grant RFBR-CERN 12-02-91532. G. Cavoto, F. Iacoangeli and R. Santacesaria acknowledge the support from MIUR (grant FIRB RBF085MOL_001/111J1000090001). S. Dabagov acknowledges the support by the Ministry of Education and Science of the Russian Federation in the frames of Competitiveness Growth Program of NRNU MEPhI, Agreement 02.A03.21.0005. Work supported by the EuCARD program GA 227579, within the ‘‘Collimators and Materials for high power beams’’ work package (Colmat-WP). The Imperial College group gratefully acknowledges support from the UK Science and Technology Facilities Council.

References

- [1] J. Lindhard, K. Dan, *Vidensk. Selsk. Mat. Fys. Medd.* 34 (14) (1965).
- [2] E.N. Tsyganov, preprint TM-682, TM-684, Fermilab, Batavia, 1976.
- [3] J.S. Forster, et al., *J. Phys. B, At. Mol. Phys.* 318 (1989) 301.
- [4] J.S. Forster, in: R.A. Carrigan Jr., J. Ellison (Eds.), *Relativistic Channeling*, Plenum Press, New York, 1987, p. 39.
- [5] W. Scandale, et al., *Phys. Lett. B* 680 (2009) 129.
- [6] W. Scandale, et al., *Phys. Lett. B* 719 (2013) 70.
- [7] W. Scandale, et al., *Phys. Rev. Lett.* 101 (2008) 234801.
- [8] S. Baricordi, et al., *Appl. Phys. Lett.* 91 (2007) 061908.
- [9] S. Baricordi, et al., *J. Phys. D, Appl. Phys.* 41 (2008) 245501.
- [10] A.M. Taratin, S.A. Vorobiev, *Sov. Phys. Tech. Phys.* 30 (1985) 927.